Polymer 51 (2010) 6115–6122

Contents lists available at ScienceDirect

Polymer

journal homepage: www.elsevier.com/locate/polymer

Mechanism and kinetics of free-radical degradation of xyloglucan in aqueous solution

Amilcar Pillay Narrainen, Peter A. Lovell*

Materials Science Centre, School of Materials, The University of Manchester, Grosvenor Street, Manchester M1 7HS, United Kingdom

ARTICLE INFO

Article history:
Received 10 August 2010
Received in revised form
21 October 2010
Accepted 24 October 2010
Available online 2 November 2010

Keywords:
Xyloglucan
Degradation
Free-radical

ABSTRACT

Free-radical degradation of xyloglucan (XG) in aqueous solution initiated by 4,4′-azobis-(4-cyanopentanoic acid), potassium persulfate (KPS), hydrogen peroxide (H_2O_2) and H_2O_2 with ascorbic acid at 75–80 °C has been investigated using gel permeation chromatography. XG degradation behaviour is similar to that of hydroxyethylcellulose with carbon-centred radicals causing little degradation and oxygen-centred radicals producing significant degradation. Based on the observations, the predominant mode of degradation is believed to be random chain scission of sterically unhindered glycosidic main-chain linkages, with an increasing contribution from side-group scission as the degree of polymerization reduces and the relative concentration of side-group linkages increases. The rate coefficient for random chain scission degradation by KPS at 75 °C was 3.98×10^{-6} s^{-1}.

1. Introduction

Xyloglucan (XG) is a structural polysaccharide that is found in the primary cell walls of higher plants [1] and commonly is used as a food additive and in the textile industry. The results presented in this paper concern a rather different use of XG and are from the first phase of an investigation into the grafting of water-soluble polysaccharides to the surfaces of polymer latex particles during emulsion polymerization. The motive for attaching polysaccharide chains to particle surfaces is twofold: (i) they can confer steric stabilization; and (ii) they are able to provide useful functionality, such as strong interaction with polar surfaces. The focus on XG in the present work is because, compared to structurally similar polysaccharides, it dissolves in water more completely to give solutions of reliably consistent properties, as will be discussed later.

The most common strategy for grafting of polysaccharides to particle surfaces during emulsion polymerization is to use initiators which generate primary radicals that are capable of abstracting a hydrogen atom from the polysaccharide backbone [2]. The resulting radical can initiate polymerization of monomer to produce a graft copolymer which, with further growth of the propagating graft, can enter an existing particle either directly or through collision following phase-separation from the aqueous medium. Alternatively, if pre-formed particles either are not present or their concentration is too low, early in the polymerization phase-separation of a propagating graft copolymer can result in creation of a primary particle that then becomes a nucleus from which fully mature particles grow. The key feature of all these processes is that they result in chemical attachment of the polysaccharide chain to the particle. The structurally similar hydroxyethylcellulose (HEC) is used widely in the emulsion polymer industry as a steric stabilizer of latex particles and has been the subject of a few studies aimed at understanding its behaviour in emulsion polymerization [3–7]. The main observations from a detailed study [3,7] were that oxygen-centred radicals, such as those produced by the dissociation of the persulfate ion, caused degradation of HEC chains in the absence of monomer, but that in the presence of acrylates, grafting to the HEC chain was favoured over degradation. Manipulation of the reaction conditions gave control of the balance between the degradation and grafting reactions and hence over the thickness of the HEC sheath attached to the particles, with important implications for the steric stabilization of the latex particles.

Hence, before attempting to synthesize XG-grafted latex particles, it was necessary to study, and gain an understanding of, XG degradation in the presence of free radicals. The results from this study are presented in this paper and are correlated with those from previously reported studies of HEC degradation.

2. Experimental

2.1. Materials

Tamarind seed xyloglucan (XG) was obtained from Dainippon Pharmaceutical Co. Ltd. All other chemicals were obtained from

* Corresponding author. Tel.: +44 161 306 3568; fax: +44 161 306 3586.
E-mail address: pete.lovell@manchester.ac.uk (P.A. Lovell).

0032-3861/$ – see front matter © 2010 Elsevier Ltd. All rights reserved.
doi:10.1016/j.polymer.2010.10.049

Aldrich and used as received: potassium persulfate (KPS) ≥99.0%, 35 wt% aqueous hydrogen peroxide (H_2O_2) solution, L-ascorbic acid (AA) ≥99.0% and 4,4′-azobis-(4-cyanopentanoic acid) (ACPA) ≥98.0%.

2.2. Preparation of aqueous solutions of XG

Several strategies were investigated for dissolution of the XG because it was not fully soluble, even when stirred in hot water. The variables investigated were: (i) type of mixer; (ii) temperature; (iii) XG concentration; and (iv) rate of addition of XG.

Two types of mixer were used. When using a Silverson L4RT high-shear mixer, the XG was added all at once into the vortex to avoid gelation, as recommended in the Silverson manual. A dis-integrating head and a square-hole, high-shear screen were investigated, both at 3000 and 6000 rpm with mixing times of approximately 5–6 min. The other mixer investigated was of much lower shear and comprised a stirrer motor fitted with a turbine impeller. This proved to be more satisfactory than the Silverson (see the Results and discussion section) and the following optimum procedure was used for preparation of the XG solutions used in the degradation studies.

Deionized water (198.3–199.8 mL) was heated at 98 °C in a round-bottom flanged reaction vessel fitted with a condenser and a radial four flat-bladed turbine impeller rotating at 600 rpm. XG (0.2–1.7 g, depending on the target solution concentration) was added to the vortex in four approximately equal aliquots over a period of 10 min using a plastic scoop to make the additions in order avoid significant absorption of water by the XG during its addition (adding the XG too fast can result in clumping, whereas adding it too slow hinders dispersion due to the viscosity increase as XG dissolves). In order to prevent shear degradation as the viscosity increased, shortly after completing the XG addition the stirrer speed was reduced to 100 rpm at which it was maintained for 30 min. The solutions were allowed to cool to ambient temperature and further deionized water was added to correct for losses due to evaporation. Separation of the insoluble material from resulting solution was achieved by centrifugation at 3000 rpm for 2 h and then removal of the clean supernatant by syringe. This procedure was highly reproducible in giving XG solutions in the concentration range 0.1–0.85 wt% with consistent properties. The solutions were stored in a refrigerator and used within two weeks of preparation. XG solution concentrations were determined by freeze-drying and weighing the dried XG.

2.3. Degradation reactions

The following procedure is representative of all degradation reactions performed, but applies to one specific reaction. Aqueous XG solution (45.0 g) was placed in a 3-neck round-bottom flask equipped with a condenser and purged with nitrogen whilst being heated to 75 °C (80 °C when using H_2O_2) in a thermostated oil bath. An aqueous solution of initiator (5.0 g) then was added to the flask, thereby defining time zero. When using the H_2O_2/AA redox couple, the AA solution was added completely first, immediately followed by complete addition of the aqueous H_2O_2 solution. Samples (ca. 3 g) were removed at selected intervals using a glass syringe fitted with a 25.4 cm stainless steel needle and immediately quenched by addition of a 1 wt% aqueous hydroquinone solution (ca. 1 g) and cooling in ice.

2.4. Brookfield viscometry

XG solution viscosities were measured at 21–22 °C using a Brookfield DV-E Viscometer with a RV-2 spindle and a rotational speed of 100 rpm.

2.5. Gel permeation chromatography (GPC)

The molar mass distribution of XG was analysed by aqueous GPC at 49 °C using 17 μm TSK-GEL G5000PW and G6000PW columns in series and a differential refractometer detector. A 0.02 wt% aqueous sodium azide solution was used as eluent at a flow rate of 0.50 mL min^{-1}. The columns were calibrated using poly(ethylene oxide) and poly(ethylene glycol) standards with molar masses in the range 194 to 996,000 g mol^{-1}. XG solutions (as prepared or removed from degradation reactions) were diluted in water (to 0.1–0.2 wt% in most cases) and passed through a 0.45 μm filter before injection.

3. Results and discussion

For mechanistic studies of degradation, it is important to know the composition and chemical structure of the monosaccharide units which constitute the polysaccharide. These usually are determined by using a combination of analytical techniques [8]. High-performance liquid chromatography and gas chromatography are used routinely to determine qualitatively and quantitatively monosaccharide composition from hydrolysed polysaccharides. Methylation analysis helps determine the position at which sugars are substituted and their abundance in the polysaccharide. The structures of component oligosaccharides can be elucidated using matrix-assisted laser desorption ionization time-of-flight mass spectrometry and using more recent techniques, such as high-performance anion-exchange chromatography. Nuclear magnetic resonance spectroscopy is another powerful tool for elucidating their composition and chemical structures. Xyloglucan samples derived from different sources have been studied using these methods [9–11].

Studies of the kinetics of degradation of polysaccharides through measurements of molar mass and molar mass distribution provide important insights into the effects of different degradation conditions and can reveal mechanistic information about the chain scission process, as will be discussed later in this paper. The most common methods employed for this type of study are gel permeation chromatography (GPC) [3,7,12–15], viscometry [13,15–17] and to a lesser extent field-flow fractionation [18].

An aqueous GPC system equipped with a differential refractometer detector was employed in this study because of its ready availability and its ability to provide complete molar mass distributions over the wide range of molar masses that needed to be accessed. XG standards were not available and so the GPC system was calibrated with poly(ethylene glycol) and poly(ethylene oxide) standards that spanned the range of molecule sizes detected for the as-supplied and partially degraded XG samples. Universal calibration procedures [19] could not be applied because the necessary Mark–Houwink–Sakurada constants were not available or measurable with the available samples and facilities. XG is expected to exist as extended rod-like or worm-like chains in aqueous solution as compared to the random coils of the standards used. Thus, for a given degree of polymerization, the XG chains will occupy a larger hydrodynamic volume than the calibration standards and so the molar masses reported herein for XG are over-estimates of their true values, though the errors will be moderated somewhat by the fact that XG is a branched polysaccharide.

3.1. XG dissolution

Tamarind seed XG has been used in the studies reported herein and comprises principally a cellulosic (β(1–4)-linked D-glucose) backbone in which some of the repeat units are substituted at position 6 with a single D-xylose residue and a disaccharide of

D-xylose and D-galactose [9,12,20]. The D-xylose residues are α (1–6)-linked to the backbone and are either terminal or substituted with β(1–2)-linked D-galactose. The D-glucose: D-xylose: D-galactose ratio has been reported to be 2.8: 2.25: 1 [9]. The branching units reduce the extent of intermolecular H-bonding as compared to cellulose and make the polysaccharide water-soluble. However, our preliminary investigations showed that, like many other sources of XG, tamarind seed XG is not completely soluble in water. Incomplete dissolution can arise from poor dispersion of wetted XG particles that can agglomerate and form gels, but dissolution is incomplete even when dispersion of the particles is done carefully, showing that there is an inherently insoluble fraction in the XG. For the degradation (and subsequent grafting) studies, it is essential to be able to prepare homogeneous XG solutions that are consistent in terms of the concentration and molar mass distribution of dissolved XG. Thus we began by evaluating different procedures for preparation of XG solutions.

The molar mass distributions of the dissolved XG were fairly similar in most cases. However, when using the high-shear Silverson mixer, a small low molar mass peak indicated that some shear degradation of the XG had occurred during the dissolution process; this peak did not disappear even when using lower mixing speeds. The relative size of this low molar mass peak was reduced by using higher temperatures due to the lower viscosity of the XG solution, but it still was not eliminated. In contrast, no such low molar mass peak was observed for XG solutions prepared using the turbine impeller at the higher temperature of 98 °C, though undissolved agglomerates could be seen when XG was added as a single addition and at ambient temperature, which gave rise to slightly lower molar mass averages and solutions of lower viscosity. The optimised procedure employed the turbine impeller and involved addition of XG to deionized water at 98 °C in four aliquots over a period of 10 min. This procedure gave XG solutions in the concentration range 0.1–0.85 wt% with very reproducible molar mass distributions.

The freeze-dried XG samples dissolved fully in hot deionized water after a few hours of gentle stirring with a magnetic bar, thus showing that insoluble impurities in the as-supplied XG are the major source of the insoluble material. The molar mass distribution of the freeze-dried XG was the same provided that the freeze-drying process was done within two weeks of XG solution preparation. However, XG solutions were found to show evidence of degradation when analysed by GPC after being stored in a refrigerator for more than two weeks, presumably due to the onset of microbial attack.

The percentage of dissolved XG (as measured by weighing freeze-dried samples) at initial concentrations of 0.65, 0.75 and 0.85 wt% in each case was 80.5 ± 1.8 wt% of the as-supplied material. The Brookfield solution viscosities and dissolved XG concentrations were highly reproducible and are given in Table 1. Although there are only three data points, over this range of concentration the solution viscosity data correlate extremely well to a straight line and so the solution viscosity provides a quick way of verifying with confidence the concentration of XG solutions in this range.

Because of limited access to a freeze dryer, the degradation studies were carried out using solutions freshly prepared at 0.75 (as-supplied) wt% XG, which typically gave a dissolved XG solution concentration of 0.60 wt% with a solution viscosity of 62–63 cP and (from GPC) a number-average molar mass (M_n) ≈ 250 kg mol^{-1} and a weight-average molar mass (M_w) ≈ 1400 kg mol^{-1}.

For comparison purposes, locust bean gum (LBG) galactomannan also was investigated. LBG has a backbone of β(1–4)-linked mannose residues that are partially substituted at position 6 by a galactose residue. There are about 3.5 mannose residues for every galactose residue making it much less substituted than XG.

Table 1
Concentrations and viscosities of the aqueous XG solutions.[a]

Concentration of dissolved XG (c)/wt%	XG solution viscosity at 21–22 °C (η)/cP
0.52	50.1 ± 0.4
0.60	62.7 ± 0.5
0.68	76.2 ± 0.3

[a] The data give the following linear least squares fit: $\eta = 163.12c - 34.875$, with a correlation coefficient of 0.9998.

Dissolution of LBG was less reliable than XG, with the presence of agglomerates of undissolved LBG visible in all the solutions produced. This is a consequence of the lower water solubility of LBG and the higher viscosity of its solutions. GPC analysis of LBG solutions separately prepared using a Silverson showed differences in molar mass distributions of the dissolved LBG, indicating that some fractions of the LBG sometimes dissolve and sometimes do not. More consistency was obtained when using the preferred turbine impeller method but the concentrations of dissolved LBG achieved still were inconsistent. For example, repeated preparation of an LBG solution (targeting 0.50 wt%), gave a wide range of percentages of dissolved LBG from 47 to 74% and, as a consequence, significantly different solution viscosities. Values of M_n and M_w were generally in the region of 350 and 2500 kg mol^{-1}, respectively. Due to the inconsistency of LBG dissolution, the kinetics of LBG degradation was investigated only briefly.

3.2. Hydrolytic stability of XG in aqueous solution

In order to be certain of the cause of XG degradation, XG solutions were investigated first in the absence of free-radical initiators under conditions that other than this would be similar to those which would be used in emulsion polymerization. In this way the contribution from hydrolytic degradation was established. The sample of XG used in this preliminary work was of slightly lower initial molar mass than the XG used in the subsequent free-radical degradation studies. The XG solutions were heated for 3 h at 75 °C under a nitrogen atmosphere both at the natural solution pH (ca. 5) and at a pH of 2.4, which replicates the acidic conditions resulting from side reactions with persulfate initiators. The molar mass distributions of the XG before and after these treatments are presented in Fig. 1 and show that under these conditions there is very little or no degradation.

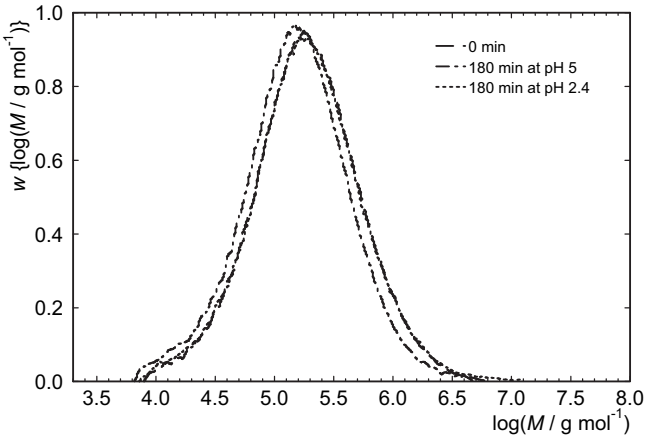

Fig. 1. Molar mass distribution of XG before and after heating at 75 °C in aqueous solution at pH ~5 (as-prepared solution) and pH 2.4.

3.3. Free-radical degradation of XG in aqueous solution

The degradation of XG was investigated in the presence of free-radical initiator systems commonly used in emulsion polymerization. In preliminary studies we found that a weight ratio of XG to KPS of 5.4 gave a rate of degradation that proceeded to a limiting extent over a period of 2–3 h, as monitored by aqueous GPC of aliquots removed during the reaction. Having established this as a suitable rate for monitoring the kinetics, when using the initiators ACPA and H_2O_2 their concentrations were adjusted to provide a similar radical flux based on calculations made using published values of initiator dissociation rate coefficients [21,22]. In order to improve its water solubility, ACPA was converted to the disodium salt by adding the required amount of sodium hydroxide solution for 100% neutralization of the carboxylic acid groups. Degradation reactions were carried out at 75 °C except for H_2O_2 which was used at 80 °C because the rate coefficient for dissociation was known at this temperature only. For the hydrogen peroxide/ascorbic acid (H_2O_2/AA) redox couple, a 5.4: 1: 3 weight ratio of XG: H_2O_2: AA was used. Previous studies have shown that this redox couple gives an initially high radical flux which, after the consumption of AA, results in a lower radical concentration [21].

By analogy with the chemistry of free-radical degradation of HEC [3–7,13,17], the expected mechanism for main-chain degradation of XG in the presence of oxygen-centred radicals (XO•) is given in Scheme 1. Thus it is proposed that degradation involves abstraction of a hydrogen atom from the cellulosic backbone by XO•. The carbon-centred radical formed then undergoes β-scission resulting in main-chain scission at the glycosidic linkage. The new radical formed can then abstract a hydrogen atom from water, generating a hydroxyl radical which can act as a chain carrier for further degradation. In studies of HEC degradation, detection of carbonyl species by UV spectroscopy supported this mechanism [7,17] and, in general, it was found that the rate of degradation depends on the molar ratio of initiator to polysaccharide and that limiting values of molar mass are obtained [7,17]. Furthermore, unlike oxygen-centred radicals, carbon-centred radicals produced from azo initiators did not give rise to significant HEC degradation under similar conditions, implying that they abstract hydrogen atoms from the cellulosic backbone at a very much lower rate [3,7,23].

The objective of the studies reported herein was to determine the rates of free-radical degradation of XG in homogeneous aqueous solution for a range of common initiators, namely, KPS, ACPA, H_2O_2 and the redox couple of H_2O_2 with ascorbic acid (AA). The approach used was to monitor changes in XG molar mass distribution by GPC and so was similar to previous studies of HEC degradation that used GPC in N,N′-dimethyl acetamide (DMAc)/LiCl [3,7] or water [13]. Due to the insolubility of XG in DMAc/LiCl and

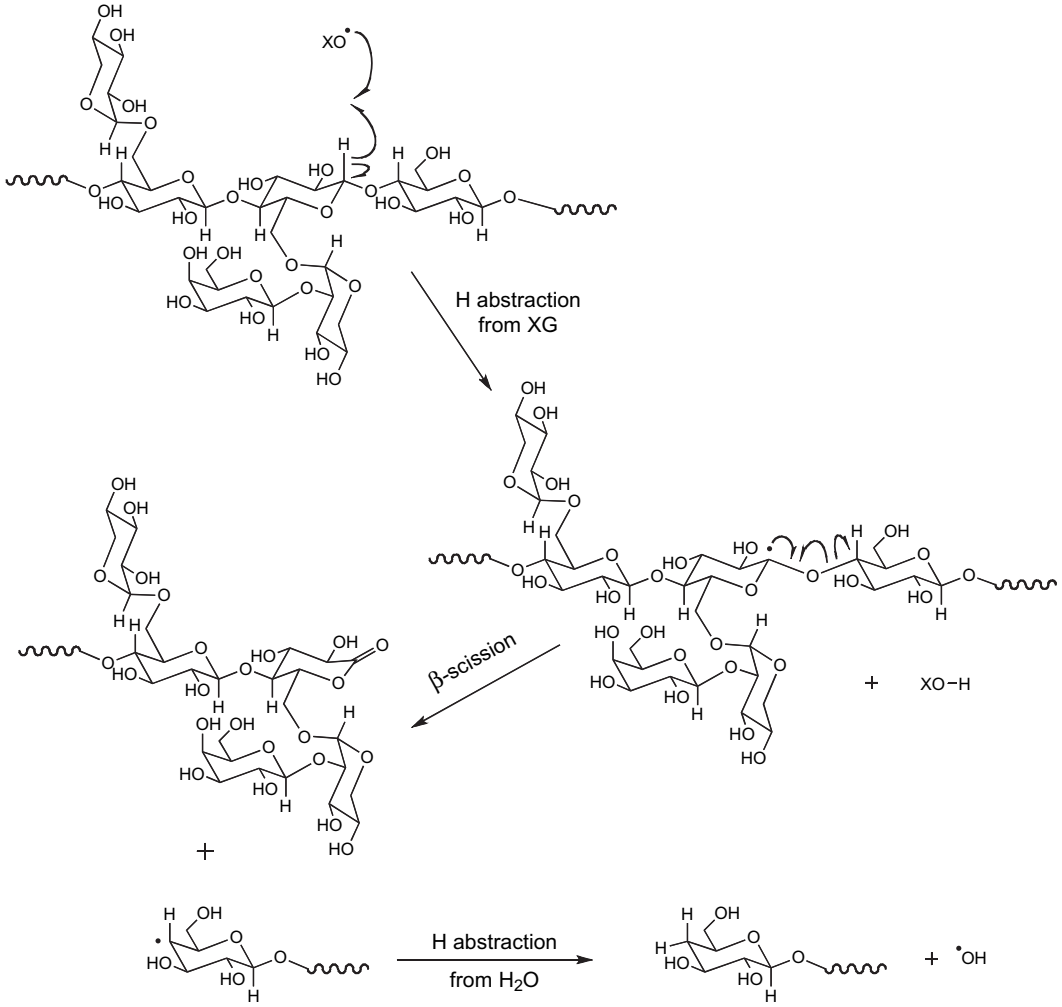

Scheme 1. Proposed mechanism for free-radical degradation of XG, exemplified by initial H abstraction at the main-chain ring C^1–H bond. Note that H abstraction at any of the main-chain ring C–H bonds can lead to main-chain scission; in the case of H abstraction at ring C^2, C^3 or C^5, β-scission first produces an enol which then tautomerizes to the keto form.

other similar polar aprotic solvents, aqueous GPC was necessary for the studies of XG degradation.

In accord with previous observations on HEC [3,7,23], use of ACPA leads to only a small amount of degradation, even after 3 h reaction (see Fig. 2). Thus carbon-centred radicals produced by the dissociation of azo initiators react only slowly with XG. In comparison, inspection of Figs. 3–5 shows that use of KPS, H_2O_2 and H_2O_2/AA leads to rapid degradation of XG, again in accord with observations on HEC which show that oxygen-centred radicals bring about rapid degradation [3–7,13,17]. Hence, our hypothesis that the mechanism of free-radical degradation of XG is similar to that of HEC is substantiated and so Scheme 1 provides a valid basis for interpretation of the results.

Considering Figs. 3–5 in more detail, it is clear that although in each case the whole molar mass distribution shifts to lower molar masses, there are significant differences between the rates of degradation. XG degradation in the presence of KPS at 75 °C (Fig. 3) proceeds smoothly, whereas when using H_2O_2 with nominally the same radical flux, though at the slightly higher temperature of 80 °C, the rate of XG degradation is low initially and accelerates after the first hour (see Fig. 4). When using H_2O_2/AA at 75 °C (Fig. 5), XG degradation proceeds rapidly with low molar masses achieved at short reaction times, most probably because both H_2O_2 and AA were added completely together at the start and undergo rapid reaction giving a very high initial radical flux.

For each of the oxygen-centred radical initiation systems, an increasing concentration of very low molar mass species is observed in the form of a shoulder in the GPC traces when M_n has reduced to about 40 kg mol^{-1}. This can be seen from Figs. 3–5 in which, at longer reaction times, the molar mass distributions of the XG samples do not return to the baseline, but instead overlap with a very low molar mass peak which also merges into the ethylene glycol flow rate marker peak. The observation is particularly prominent in the H_2O_2/AA reaction, as is evident from the overlay of GPC traces for degradation of XG with H_2O_2 at 80 °C shown in Fig. 6 and is presumed to be due to release of monomeric or dimeric sugar residues. Only the main GPC peaks have been analysed when determining M_n from the molar mass distributions shown in Figs. 3–5 (i.e. by integrating down to the molar mass at which the low molar mass upturn in the molar mass distribution occurs, i.e. at approximately 2.0 kg mol^{-1}). Since M_n is sensitive to placement of the baseline, especially at the low molar mass end of the distribution, this will result in significant errors in the values of M_n determined for those samples which show the additional peak at very low molar mass. However, the earlier samples, where M_n is changing rapidly, are most important for fitting of the data to random chain scission theory (see later) and their M_n values could be determined with confidence because of the well-defined baselines at high and low molar mass in their GPC traces. Fry and co-workers studied the non-enzymatic degradation of XG by hydroxyl radicals in the presence of oxygen [16,24,25]. By labelling the sugar residues that have been attacked by free radicals, but which did not result in scission, they found that the galactose residue is the most prone to attack, and that xylose residues also are much more susceptible to attack than the glucose backbone, taking into account the relative proportions of the sugar moieties in the repeat unit [24]. However, their measurements were made on the final samples after long degradation times and they also could be interpreted as implying that attack of side-groups is favoured after predominant initial attack on unhindered main-chain linkages. Hence, a possible explanation for our observation of an increasing amount of monomeric or dimeric sugar residues as the XG degradation progresses is that the XG side-groups are less susceptible to radical attack than the unhindered glycosidic linkages in the main-chain (see Scheme 1). As random degradation of the main-chain proceeds, the proportion of side-group glycosidic linkages in the chain increases, resulting in an increased probability of attack by free radicals; as a consequence, a non-Gaussian molar mass distribution begins to develop and side-chain sugar moieties

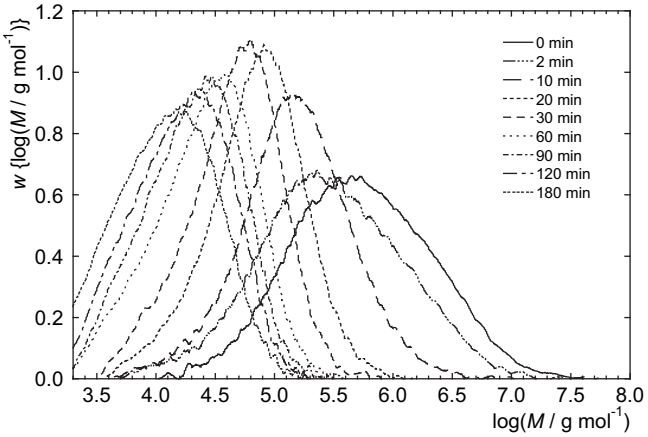

Fig. 3. Evolution of molar mass distribution with time for free-radical degradation of XG in 0.54 wt% aqueous solution at 75 °C with 3.70 mmol dm^{-3} KPS as initiator.

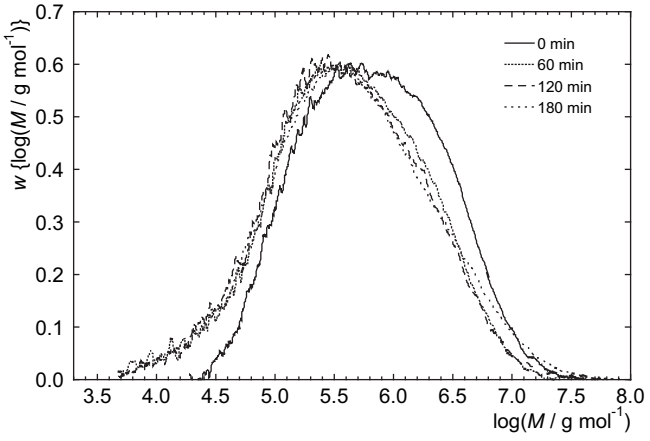

Fig. 2. Evolution of molar mass distribution with time for free-radical degradation of XG in 0.54 wt% aqueous solution at 75 °C with 2.31 mmol dm^{-3} ACPA disodium salt as initiator.

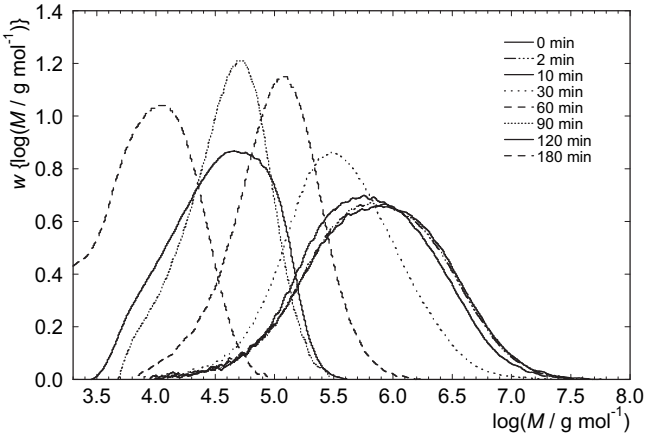

Fig. 4. Evolution of molar mass distribution with time for free-radical degradation of XG in 0.54 wt% aqueous solution at 80 °C with 124.4 mmol dm^{-3} H_2O_2 as initiator.

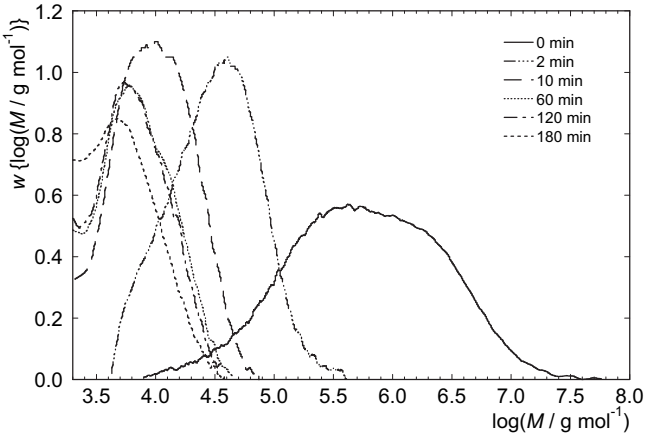

Fig. 5. Evolution of molar mass distribution with time for free-radical degradation of XG in 0.54 wt% aqueous solution at 75 °C with 29.4 mmol dm^{-3} H_2O_2 and 16.4 mmol dm^{-3} AA as initiator.

become increasingly more prominent in the GPC traces during the later stages of XG degradation.

3.4. Kinetics of free-radical degradation of XG in aqueous solution

Assuming that XG degradation proceeds mainly by scission of equivalent main-chain linkages, the variation of M_n with reaction time can be analysed as a random scission process. Fig. 7 compares the evolution of M_n and M_w/M_n for the reactions with KPS, H_2O_2 and H_2O_2/AA. Random chain scission theory predicts that as the number of chain scissions increases the molar mass distribution of the residual polymer will steadily approach the form of the most probable distribution with $M_w/M_n = 2$ regardless of the form of the original molar mass distribution. Although, as discussed in the previous section, the XG molar mass distributions generally lose their monomodal nature at high extents of degradation, M_w/M_n for the main GPC peak is generally about 2 after significant degradation for all three reactions. Hence, analysis of the results using random chain scission theory is justified.

If chain scission is first order with respect to the number of main-chain linkages, the following integrated kinetics equation for random chain scission can be applied [14].

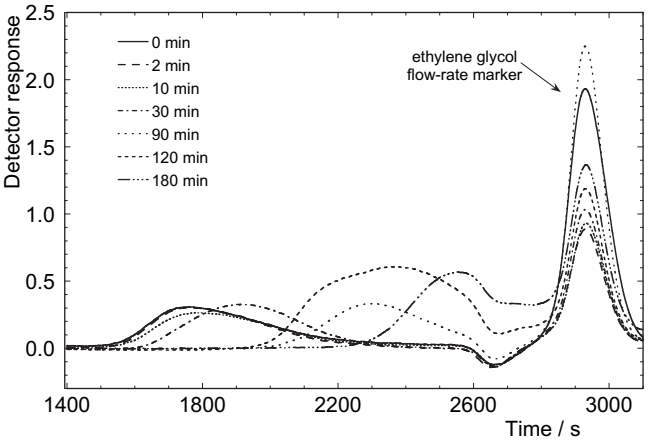

Fig. 6. GPC chromatograms of detector response against time for samples removed during free-radical degradation of XG in 0.54 wt% aqueous solution at 80 °C with 124.4 mmol dm^{-3} H_2O_2 as initiator.

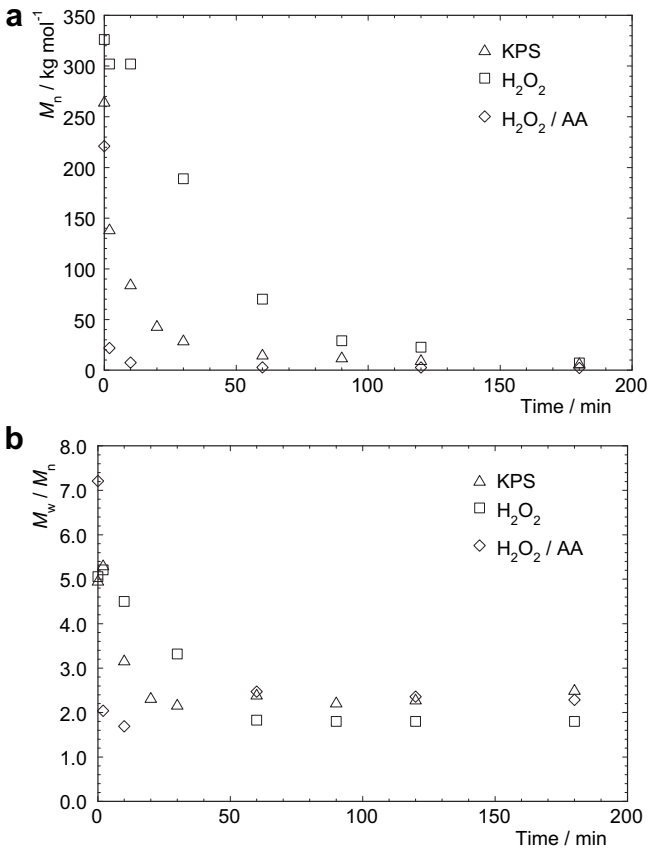

Fig. 7. Variation of (a) number-average molar mass, M_n, and (b) polydispersity index, M_n/M_w with time for free-radical degradation of XG in 0.54 wt% aqueous solution using as initiator: KPS at 75 °C; H_2O_2 at 80 °C; and H_2O_2/AA at 75 °C.

$$\log\left(1-\frac{1}{(x_n)_t}\right)-\log\left(1-\frac{1}{(x_n)_0}\right)=-kt \tag{1}$$

where k is the rate coefficient for main-chain scission, and $(x_n)_0$ and $(x_n)_t$ are, respectively, the XG number-average degree of polymerization before degradation and after degradation for time t. For large values of x_n the logarithmic terms in Equation (1) can be expanded to give the simplified expression

$$\frac{1}{(x_n)_t}-\frac{1}{(x_n)_0}=kt \tag{2}$$

Recognising that $M_n = x_n M_0$ where M_0 is the mean XG repeat unit molar mass (326.1 g mol^{-1} for tamarind seed XG), Equation (2) can be cast into a more convenient form in order to use M_n values obtained from GPC analysis.

$$\frac{1}{(M_n)_t}-\frac{1}{(M_n)_0}=\frac{kt}{M_0} \tag{3}$$

where $(M_n)_0$ and $(M_n)_t$ are, respectively, the XG number-average molar mass before degradation and after degradation for time t. Thus a plot of $\{1/(M_n)_t - 1/(M_n)_0\}$ against t will give a straight line with slope k/M_0. This idealised relationship has been applied to the thermal degradation of cellulose [14] and to the free-radical degradation of HEC [7] with the linear relationship observed principally during the initial stages of degradation. An assumption inherent in Equation (1), and hence in Equation (3), is that the rate of radical formation is approximately constant during the period of the degradation experiments (so that degradation can be treated as

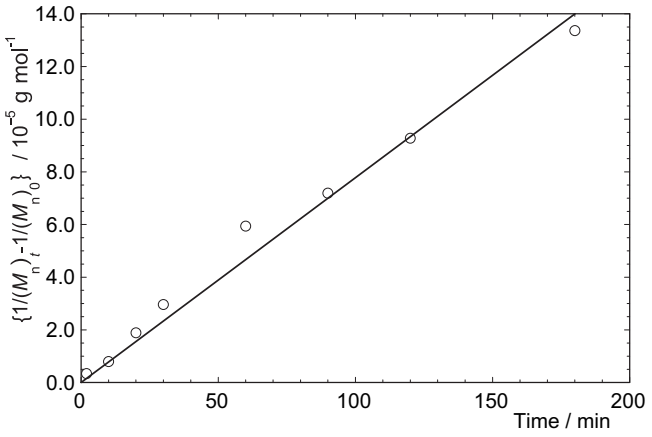

Fig. 8. Plot of $\{1/(M_n)_t - 1/(M_n)_0\}$ against time for free-radical degradation of XG in 0.54 wt% aqueous solution at 75 °C with 3.70 mmol dm^{-3} KPS as initiator.

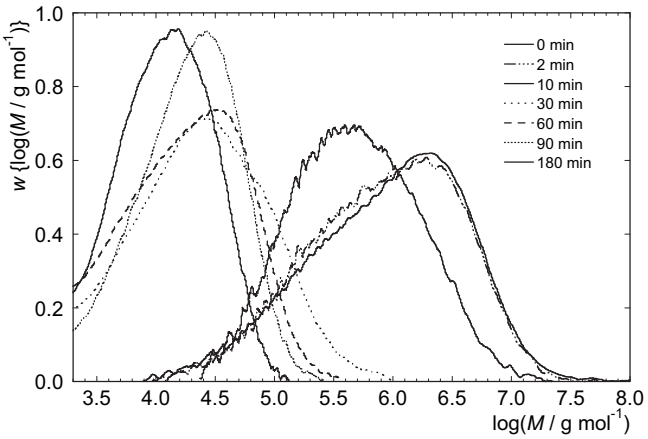

Fig. 10. Evolution of molar mass distribution with time for free-radical degradation of LBG in a target 0.75 wt% aqueous solution at 75 °C with 3.70 mmol dm^{-3} KPS as initiator.

a pseudo first-order process). Given that the reduction in M_n is rapid, this assumption is reasonable for degradation involving thermal decomposition of KPS and H_2O_2 under the conditions used (their corresponding half-lives being 4.8 h [26] and 144 h [21], respectively), but it is likely to be invalid for the degradation reaction using the H_2O_2/AA redox couple. Hence only the data from XG degradation using thermal decomposition of KPS and H_2O_2 have been analysed using Equation (3).

Fig. 8 shows a linear regression plot according to Equation (3) for the degradation of XG with KPS. The data fit well to the equation indicating that degradation initiated by KPS is quite simple and governed by a single rate coefficient with $k/M_0 = 1.22 \times 10^{-8}$ mol g^{-1} s^{-1}, which gives $k = 3.98 \times 10^{-6}$ s^{-1}. This value compares well with $k = 3.00 \times 10^{-6}$ s^{-1} ($k/M_0 = 1.10 \times 10^{-8}$ mol g^{-1} s^{-1}) determined for degradation of HEC (Natrosol 250 LR and 250 GR) in aqueous solution at 80 °C with ammonium persulfate (APS) at similar molar ratios of repeat units to initiator (4.2 compared to 4.5 for XG in the present study) [7], thus providing further evidence for the similarity of free-radical degradation of XG and HEC, as proposed in Scheme 1.

Degradation of a target 0.75 wt% LBG solution showed characteristics similar to XG degradation with the same weight ratio of KPS to polysaccharide: (i) as can be seen in Fig. 9, a second peak in the GPC curves appeared at lower molar mass later in the reaction (again indicating side-chain scission); and (ii) the polydispersities of the degraded LBG approached 2 (suggesting a random scission process). However, the degradation of LBG was initially slower, but accelerated after about 10 min reaction (see Fig. 10) and so, unlike XG degradation, the M_n data could not be analysed quantitatively because they did not fit well to Equation (3). The reasons for this are not clear, but it may be that some of the LBG was still not completely in solution at the start of the reaction and so less accessible to attack by sulfate radical-anions.

In contrast to degradation due to KPS, analysis of the data for degradation of XG with H_2O_2 according to Equation (3) reveals an increasing rate (see Fig. 11). In view of this difference, the H_2O_2 degradation experiment was repeated, which showed that the observations were reproducible and, hence, real. The more substantial increase in rate of XG degradation after 1 h correlates with the appearance of the very low molar mass species in the GPC traces (see Fig. 6). Hence a plausible explanation of the increasing rate of degradation with H_2O_2 is that as the degradation progresses, the concentration of reducing sugars formed by scission of side-groups increases and that they undergo a redox reaction with H_2O_2 thereby increasing the rate of H_2O_2 decomposition.

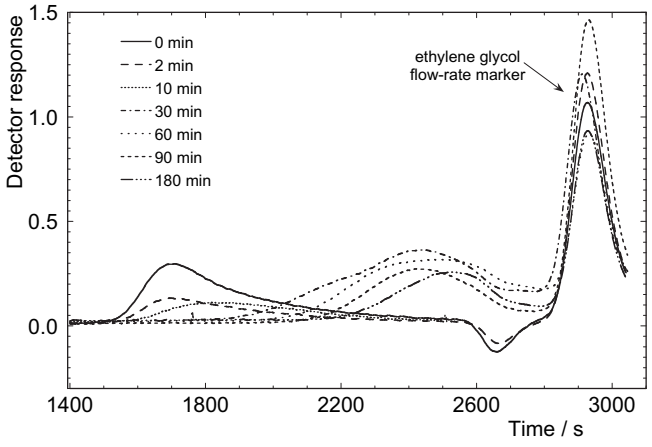

Fig. 9. GPC chromatograms of detector response against time for samples removed during free-radical degradation of LBG in a target 0.75 wt% aqueous solution at 75 °C with 3.70 mmol dm^{-3} KPS as initiator.

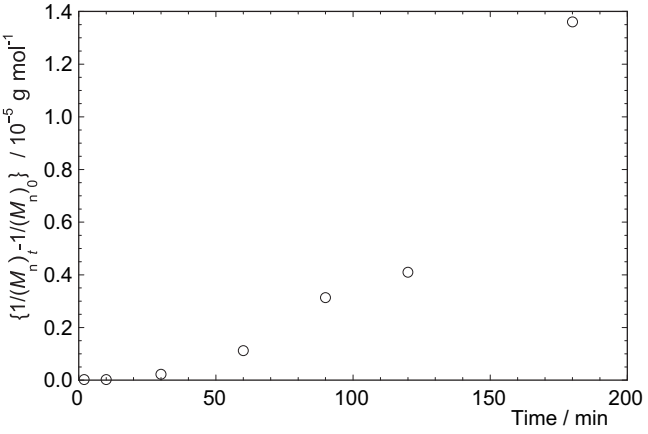

Fig. 11. Plot of$\{1/(M_n)_t - 1/(M_n)_0\}$ against time for free-radical degradation of XG in 0.54 wt% aqueous solution at 80 °C with 124.4 mmol dm^{-3} H_2O_2 as initiator.

The initial rate of XG degradation with H_2O_2 is significantly lower than with KPS even though the initial rates of radical formation were calculated to be the same and the XG degradation with H_2O_2 was performed at the slightly higher temperature (80 vs 75 °C). This implies that the sulfate radical-anion has an inherently higher rate of H abstraction from the cellulosic backbone, such that a higher concentration of hydroxyl radicals from H_2O_2 would be required to match the rate of H abstraction achieved with persulfate.

Degradation of XG with H_2O_2/AA proceeded very rapidly and distinct molar mass distributions relating to a random scission process were not obtained. Thus, the data were not suitable for plotting according to Equation (3). A reduction in the concentration of either H_2O_2 or AA or the slow addition of either component would, therefore, be expected to reduce the rate of degradation and provide greater control over molar masses.

4. Conclusions

Homogeneous aqueous XG solutions show free-radical degradation behaviour similar to HEC: (i) use of carbon-centred radicals from an azo initiator does not bring about significant degradation, whereas oxygen-centred radicals from KPS and H_2O_2 result in reasonably rapid degradation, and (ii) the rate coefficient for degradation of XG by persulfate is close to that determined for degradation of HEC under similar conditions. As expected, the rate of XG degradation by H_2O_2 increases significantly on increasing the radical flux by addition of ascorbic acid. Thus, the results support the mechanism of XG degradation presented in Scheme 1. Random chain scission of sterically unhindered glycosidic linkages of the cellulosic backbone of XG is believed to be the predominant mode of degradation during the early stages with an increasing contribution from side-group scission as the degree of polymerization reduces and the relative concentration of side-group linkages increases.

The results presented in this paper provide a strong foundation for understanding the kinetics of degradation of XG in aqueous media and have informed our studies of the effects of added monomer on XG degradation, the occurrence of grafting to XG, and grafting of XG to latex particle surfaces during emulsion polymerization. The results from those studies will be presented in a subsequent paper.

Acknowledgements

The authors wish to acknowledge the Department for Business Enterprise and Regulatory Reform (BERR; formerly known as the Department of Trade and Industry DTI), for funding this work and to thank their industrial collaborators at Unilever and Synthomer for their assistance in the research. Mr. Keith Nixon of the School of Chemistry at The University of Manchester is thanked for help and support in using the aqueous GPC equipment.

References

[1] York WS, Harvey LK, Guillen R, Albersheim P, Darvill AG. Carbohydr Res 1993;248:285.
[2] Jenkins DW, Hudson SM. Chem Rev 2001;101(11):3245.
[3] Annable T, Gray I, Lovell PA, Richards SN, Satgurnathan G. Prog Colloid Polym Sci 2004;124:159.
[4] Craig DH. Polym Mat Sci Eng 1985;53:529.
[5] Craig DH. Polym Mat Sci Eng 1986;55:486.
[6] Craig DH. Grafting reactions of hydroxyethylcellulose during emulsion polymerization of vinyl monomers. In: Glass JE, editor. Water-soluble polymers: beauty with performance, vol. 213. Washington DC: ACS; 1986. p. 351.
[7] Gray I. Grafting of acrylic monomers to hydroxyethylcellulose during emulsion polymerisation. PhD thesis. UMIST; 2001.
[8] Chaplin MF, Kennedy JF. Carbohydrate analysis: a practical approach. 2nd ed. IRL Press; 1994.
[9] Gidley MJ, Lillford PJ, Rowlands DW, Lang P, Dentini M, Crescenzi V, et al. Carbohydr Res 1991;214(2):299.
[10] Aboughe-Angone S, Nguema-Ona E, Ghosh P, Lerouge P, Ishii T, Ray B, et al. Carbohydr Res 2008;343(1):67.
[11] Chattopadhyay K, Ghosh P, Ghosal P, Ray B. Indian J Chem Sect B Org Chem Incl Med Chem 2007;46B(3):471.
[12] Vodenicarova M, Drimalova G, Hromadkova Z, Malovikova A, Ebringerova A. Ultrason Sonochem 2006;13(2):157.
[13] Erkselius S, Karlsson OJ. Carbohydr Polym 2005;62(4):344.
[14] Emsley AM, Stevens GC. Cellulose 1994;1(1):26.
[15] Hsu S-C, Don T-M, Chiu W-Y. Polym Degrad Stab 2001;75(1):73.
[16] Fry SC. Biochem J 1998;332:507.
[17] Donescu D, Gosa K, Diaconescu I, Carp N, Mazare M. Colloid Polym Sci 1980;258:1363.
[18] Moon MH, Shin DY, Lee N, Hwang E, Cho I-H. J Chromatogr B Analyt Technol Biomed Life Sci 2008;864(1–2):15.
[19] Grubisic Z, Rempp P, Benoit H. J Polym Sci B Polym Lett 1967;5:753.
[20] Reis D, Vian B, Darzens D, Roland JC. Planta 1987;170(1):60.
[21] Schneider M, Graillat C, Boutti S, McKenna TF. Polym Bull 2001;47(3–4):269.
[22] Blackley DC, Haynes AC. J Chem Soc Faraday Trans 1979;75:935.
[23] Craig DH. Polym Mat Sci Eng 1986;54:370.
[24] Miller JG, Fry SC. Carbohydr Res 2001;332(4):389.
[25] Tabbi G, Fry SC, Bonomo RP. J Inorg Biochem 2001;84(3–4):179.
[26] Kolthoff IM, Miller IK. J Am Chem Soc 1951;73:3055.